Synthetizing hydrodynamic turbulence from noise: Formalism and applications to Plankton dynamics

F. Sagués and R. Reigada[*], J.M. Sancho[†], R.M. Hillary[**] and M.A. Bees[‡]

[*] *Departament de Química Física, Universitat de Barcelona, Diagonal 647, 08028 Barcelona, Spain*
[†] *Departament d'Estructura i Constituents de la Matèria, Facultat de Física, Universitat de Barcelona, Diagonal 647, 08028 Barcelona, Spain*
[**] *Department of Mathematics and Statistics, University of Surrey, GU2 7HX, UK*
[‡] *Department of Mathematics, University of Glasgow, G12 8QW, UK*

Abstract. We present an analytical scheme, easily implemented numerically, to generate synthetic Gaussian 2*D* turbulent flows by using linear stochastic partial differential equations, where the noise term acts as a random force of well-prescribed statistics. This methodology leads to a divergence-free, isotropic, stationary and homogeneous velocity field, whose characteristic parameters are well reproduced, in particular the kinematic viscosity and energy spectrum. This practical approach to tailor a turbulent flow is justified by its versatility when analizing different physical processes occurring in advectely mixed systems. Here, we focuss on an application to study the dynamics of Planktonic populations in the ocean.

INTRODUCTION.

Ideally, the statistical properties [1, 2] of any turbulent flow should come as the output of a first principles, Navier-Stokes based, formulation of the problem. However, we will adopt here a somewhat reversed perspective aimed at developing a methodology to construct what would be a sort of synthetic turbulence [3]. Rather than to retain the nonlinear coupling which makes possible the redistribution of energy from the largest length scales down into the smaller ones, we assume that the energy is incorporated into the system in an individual wave number basis, to reproduce the desired energy spectrum distribution of the turbulent flow in steady state.

The generation of the flow field proceeds from the two-dimensional simulation of a Langevin equation for the stream function $\eta(\mathbf{r},t)$,

$$\frac{\partial \eta(\mathbf{r},t)}{\partial t} = \nu\nabla^2\eta(\mathbf{r},t) + Q[\lambda^2\nabla^2]\nabla\cdot\zeta(\mathbf{r},t), \tag{1}$$

where ν stands for the kinematic viscosity and $Q[\lambda^2\nabla^2]$ denotes an operator which controls the spatial structure of the flow, with λ standing for its typical correlation length. Furthermore, $\zeta(\mathbf{r},t)$ represents a Gaussian white-noise field with zero mean value and whose covariance is given by

$$\left\langle \zeta^i(\mathbf{r}',t')\zeta^j(\mathbf{r}'',t'')\right\rangle = 2\varepsilon_0\nu\delta(t'-t'')\delta(\mathbf{r}'-\mathbf{r}'')\delta^{ij} \tag{2}$$

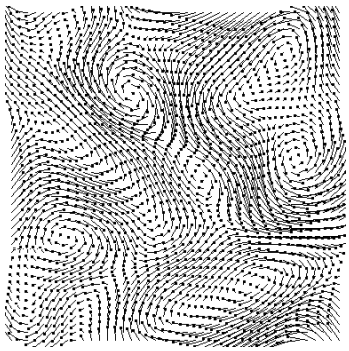

FIGURE 1. Snapshot of the “frozen" turbulent velocity field employed in the simulations in this study.

where ε_0 is the parameter that determines the intensity of the noise and further on that of the mimicked turbulent flow. This Langevin equation can be formally integrated in Fourier space to get the temporal evolution of the stream function. The incompressible two-dimensional discretized velocity field $\mathbf{U}_{i,j}$ follows from the stream function

$$\mathbf{U}_{i,j}(t) = \mathbf{U}(\mathbf{r}_{i,j},t) = \left(-\frac{\partial \eta(\mathbf{r}_{i,j},t)}{\partial y}, \frac{\partial \eta(\mathbf{r}_{i,j},t)}{\partial x} \right). \tag{3}$$

This synthetic fluid flow is characterized by three basic well-defined statistical properties; u_0^2 as the intensity of the flow, l_0 as the length correlation of the flow and t_0 as the time correlation of the flow [3]. These flow parameters are defined in terms of the velocity correlation function, which in turn, is formally associated to the energy spectrum (that depends on the form of the operator Q), and explicitly on the input parameters ν, ε_0, and λ. In this contribution we consider for most of the applications a flow with the Kraichnan spectrum [4]. In this case $E(k)$ in $2D$ is given by $E(k) \propto k^2 exp\left(-k^2/k_0^2\right)$ and correspondingly the diferential operator Q adopts the form $Q[\lambda^2\nabla^2] = exp(\lambda^2\nabla^2/2)$.

Although the general method of flow generation allows us to work with a non-stationary field, we shall not make use of the possibility in this study. For the sake of simplicity, and in order to avoid the existence of a great number of temporal scales, we take a stationary flow, and so fix $t_0 = \infty$ in the flow simulations. As an example, in Fig. 1 we show the flow realization used in this work. This flow has been generated using a square lattice of 128×128 points, and l_0 corresponds to a tenth of the linear size of the grid.

This model of synthetic turbulence has been used to study a large number of physical processes. Examples to be considered include dispersion of passive[5] and non-passive[6] particles, either reactive[7, 8] or non-reactive, front propagation phenomena[9] or phase-separating mixtures[10]. In this work we present an application to the study of planktonic populations in the ocean.

TURBULENT ADVECTION. INERTIAL EFFECTS.

When describing the motion of advected planktonic organisms or, in general any kind of non-passive particles, inertial effects due to their viscous and inertial properties have to be considered. In a Lagrangian prescription (the most visual and direct approach to study particle advection), the equation of motion for a spherical particle was derived by Maxey & Riley [11],

$$m_p \frac{d\mathbf{V}_n}{dt} = m_f \frac{D\mathbf{U}(\mathbf{X}_n)}{Dt} + 6\pi a\mu(\mathbf{U}(\mathbf{X}_n) - \mathbf{V}_n) - \frac{m_f}{2}\left(\frac{d\mathbf{V}_n}{dt} - \frac{d\mathbf{U}(\mathbf{X}_n)}{dt}\right) - 6\pi a^2\mu \int_{-\infty}^{t} \frac{d(\mathbf{V}_n - \mathbf{U}(\mathbf{X}_n))/d\tau}{\sqrt{\pi\nu(t-\tau)}} d\tau, \quad (4)$$

being $\mathbf{X}_n$ the position of the particle n with velocity $\mathbf{V}_n$, in a velocity field, $\mathbf{U}(\mathbf{X}_n)$. m_p and m_f are the particle and fluid masses respectively, μ and ν are the dynamic and kinematic viscosities associated with the surrounding fluid and a is the radius of the particle. In Eq.(4) we have distinguished between two different derivative terms, D/Dt and d/dt. The first corresponds to the material derivative following a fluid element whereas the second denotes the derivative following the particle in the fluid such that $d\mathbf{U}/dt = \partial\mathbf{U}/\partial t + [\mathbf{V}_n \cdot \nabla]\mathbf{U}$. The first term in Eq. (4) is the Bernoulli term which is the force from the undisturbed flow, the second term is the Stokes viscous drag, the third is the added mass term and the final term is the Basset history force. This equation assumes that the particle, associated Reynolds number and fluid gradients around the particle surface are small [11]. Hereafter we consider that the drag and inertia terms are dominant and the particle is small, so that the history term can be neglected. We simplify even more the equation of motion assuming that the work done displacing a fluid element must be dependent on the forces on the fluid at that point. According to this idea we exchange the particle derivative for the fluid derivative in the added mass term to obtain a reduced version of Eq. (4) that reads [6, 11]

$$\frac{d\mathbf{V}_n}{dt} = A(\mathbf{U}(\mathbf{X}_n) - \mathbf{V}_n) + R\frac{D\mathbf{U}(\mathbf{X}_n)}{Dt}. \quad (5)$$

In this equation we have non-dimensionalized the time by rescaling it using the flow timescale l_0/u_0. We have defined $A = \alpha l_0/u_0$ as the dimensionless version of the inertia parameter $\alpha = (12\pi a\mu)/(2m_p + m_f)$, that corresponds to the balance between the viscous and inertial forces. The Bernouilli parameter $R = 3m_f/(2m_p + m_f)$ is the ratio between masses.

Eq. (5) can not be solved analytically, but it is possible to obtain reliable information from it in the limit where the viscous term dominates ($A > 1$). This asymptotic analysis was introduced by Maxey [12] for the singular case of infinitely heavy particles and extended to the general case for some of us [6]. It amounts to formally integrate the particle motion according to Eq. (5) under the assumption that A is large, so that exponential transients can be eliminated, and retain only terms up to the first order in A^{-1}. If we assume that the ambient flow is stationary, we have the following expression

for the effective velocity field, $\mathbf{V}(\mathbf{r})$:

$$\mathbf{V}(\mathbf{r}) = \mathbf{U}(\mathbf{r}) + \frac{R-1}{A}\left[\mathbf{U}(\mathbf{r})\cdot\nabla\right]\mathbf{U}(\mathbf{r}) + \mathscr{O}(A^{-2}). \tag{6}$$

Actually, the above approximation assumes that the particle velocities adapt instantaneously to that of the surrounding fluid flow, and are only determined by the particle positions, neglecting the impact of trajectory memory. This is guaranteed by assuming that the viscous forces dominate the other ones. This allows the construction of an effective particle velocity field $\mathbf{V}(\mathbf{r})$ that closely matches the physical particle dynamics, and that can be easily implemented in a Eulerian formalism as we shall do later.

The most relevant signature of nonpassive advection is that particles drift from the flow trajectories due to inertia and tend to aggregate in various zones depending on their material characteristics [6, 12]. The aggregation of particles occurs in regions of negative divergence, $\nabla\cdot\mathbf{V} < 0$, in contrast to neutrally buoyant, passively advected particles. The divergence of the velocity $\mathbf{V}$ in Eq. (6) can be written in terms of the squares of the magnitudes of the local strain rate and the local vorticity, $\mathscr{S}^2$ and $|\Omega|^2$, respectively, of the original turbulent flow, $\mathbf{U}$, as follows

$$\nabla\cdot\mathbf{V} = \frac{R-1}{A}\left(2\mathscr{S}^2 - \frac{|\Omega|^2}{2}\right), \tag{7}$$

which leads to two different possibilities for aggregation. If the particle is heavier than the fluid ($R<1$) then accumulation occurs in regions where $\mathscr{S}^2 > |\Omega|^2/4$, regions of high strain and low vorticity. Conversely, if a particle is lighter than the surrounding medium ($R>1$) accumulation occurs in regions where $\mathscr{S}^2 < |\Omega|^2/4$, areas with high vorticity and low strain.

KINETIC MODEL FOR PLANKTON DYNAMICS

The versatility of our synthetic turbulence has allowed us to explore several physical systems in which the advection plays a crucial role. As anticipated, here we focus on the study of the influence of turbulent advection in Planktonic populations. Plankton patchiness has been observed on a wide range of spatial and temporal scales [13, 14, 15] and has been attributed to a range of physical and biological mechanisms. It is important to understand both the mechanisms that result in patchiness and the effect of patchiness on food-web interactions, which can have a major impact on fisheries policy.

Besides, at moderate spatial scales phytoplankton “blooms" can occur, whereby the population of phytoplankton rapidly increases in number and remains at this level for some period of time before returning to normal. This is the hallmark of an excitable system. Truscott & Brindley [16] investigated a two component phytoplankton-zooplankton (PZ) model which has the characteristics of an excitable system whose excitability is robust over a realistic parameter range. Normally, however, a large driving perturbation is required to initiate the bloom. Many mechanisms such as variations in salinity, temperature and nutrient mixing have been proposed to explain this initiation. In this work, we explore the effects of inertia in complex flows on excitable PZ dynamics. In particular,

we shall address the question of whether the inertial separation of phytoplankton and zooplankton is sufficient to seed a bloom.

We propose the following system of reaction-advection-diffusion equations to represent the effects of planktonic interactions and diffusion in an Eulerian frame:

$$\frac{\partial P}{\partial t} = -\nabla\cdot(\mathbf{V}^P P - D_P \nabla P) + rP\left(1-\frac{P}{K}\right) - \frac{\gamma Z P^2}{P^2+\kappa^2},$$
$$\frac{\partial Z}{\partial t} = -\nabla\cdot(\mathbf{V}^Z Z - D_Z \nabla Z) + \frac{e\gamma Z P^2}{P^2+\kappa^2} - \delta Z, \tag{8}$$

where $\mathbf{V}^i$ represents the velocity, with inertial and viscous corrections, of species i subject to advection by the flow obtained from Eq. (5), at lengthscales above the grid size, and grid-scale diffusive effects due to turbulent diffusion, with diffusivities D_P and D_Z. The last two terms in Eq. (8) correspond to the phytoplankton and zooplankton interactions following the excitable system proposed by Truscott & Brindley [16], which in essence models logistic phytoplankton growth, Holling type III grazing by zooplankton and a linear higher-predatory response with regard to the zooplankton mortality.

We non-dimensionalize Eq. (8) such that $P = Kp$, $Z = Kz$, $x = l_0\tilde{x}$, $y = l_0\tilde{y}$, $t = \tau l_0/u_0$, $\mathbf{V}^i = u_0\mathbf{v}^i$. After dropping the tildes this gives us the following non-dimensional version of Eq. (8),

$$\frac{\partial p}{\partial \tau} = -\nabla\cdot(\mathbf{v}^p p - d_p\nabla p) + \beta p(1-p) - \frac{\bar{\gamma} z p^2}{p^2+\chi^2},$$
$$\frac{\partial z}{\partial \tau} = -\nabla\cdot(\mathbf{v}^z z - d_z\nabla z) + \varepsilon\left(\frac{\bar{\gamma} z p^2}{p^2+\chi^2} - \sigma z\right), \tag{9}$$

where the dimensionless parameters are defined to be $\beta = rl_0/u_0$, $\varepsilon = e$, $\chi = \kappa/K$, $\sigma = \delta l_0/(\varepsilon u_0)$, $\bar{\gamma} = \gamma l_0/u_0$, $d_i = D_i/(u_0 l_0)$.

We choose L, the simulation box size, to be 100 km, the length scale of the eddies $l_0 \approx L/10$), and the characteristic velocity to be $u_0 = 0.075$ m s^{-1}, similar to that used in both Abraham [14] and Neufeld *et al.* [17]. From Truscott & Brindley [16], we take $\beta = 0.43$, $\chi = 0.053$, $\sigma = 0.34$ and $\varepsilon = 0.04$ (hence, the zooplankton population is the slow-recovery variable). Our choice of l_0 and u_o are such that we can realistically fix $\bar{\gamma} = 1$ and, hence, the reaction effects are comparable to advective effects. Kraichnan's spectrum has a maximum occurring at $k = 0.75$ and drops to a very small value at $k = 2$. Hence, the lengthscale associated with the highest energy is equal to 2 π / 0.75 = 8.4, or about a tenth of the length of the simulation region. The lengthscale associated with a wavenumber of 2 (residual energy) is given by 2 π / 2 = π, or about one 20th of the simulation region. If the simulation region is 100 km then the dimensional lengthscale associated with low spectral energy is $L/20 = 5\times10^5$ cm. This is the lengthscale for which we wish to implement a turbulent diffusivity in the reaction-advection-diffusion system. Hence, the diffusivity $D = 0.01 * l^{1.15} = 4\times10^4$ cm^2 s^{-1} = 4 m^2 s^{-1} (according to the empirical relationship extracted by Okubo [18] from experimental data). Therefore, the synthetic turbulence accounts for the large scale flow centered around a wavenumber k_0.

The system is spatially discretized using a square lattice of 128×128 cells, with a grid spacing of 0.5, and the time step used in the numerical scheme is $\Delta t = 0.001$. The integration of Eq. (9) was achieved by using a two-step *Lax-Wendroff* scheme which gave good numerical convergence for the parameter values employed. Simultaneously, we integrate Eq. (5) to obtain the velocities $\mathbf{V}^i$. We use the same $A = 6$ ($\gg 1$) for both species, but different Bernouilli parameters, R_p and R_z.

We begin from a homogeneous initial distribution of both species in their unexcited, equilibrium concentration values $p^* = 0.04589$ and $z^* = 0.04379$. The inertial separation under turbulent advection is enough to perturb the equilibrium distribution and, analogous to the threshold nature of perturbations in excitable systems, we find that there exist critical values of the Bernoulli parameters which separate regimes where no bloom occurs from regions where localized excitation and subsequent bloom propagation results.

First, we consider the extreme inertial regime, $R_p = 1.2$ and $R_z = 0.8$; namely, very light phytoplankton and very heavy zooplankton. As the phytoplankton accumulate in the eddies, the population locally exceeds the threshold value and excitation begins. Diffusion allows the excitation to move out from the eddies but the flow eventually forces this wave back into the vortices. At the same time the excitation decays and these three processes reach a steady, heterogeneous distribution of plankton, with phytoplankton at the excited state inside the eddies and below it outside. The pulse propagation is also tempered by the dilutory effects of the non-zero flow divergence enforced by inertial advective effects coupled with the geometry of the domain.

The most interesting scenario occurs for the regime where we have neutrally buoyant phytoplankton ($R_p = 1$) and slightly heavy zooplankton ($R_z = 0.95$). Here, we see the emergence, again without need of an inertial excitation, of an oscillatory bloom in the average phytoplankton population with a period of around one year, which is interesting in view of the annual nature of the observed blooms (although seasonal forcing is likely to have a major role). Fig. 2 presents the spatial evolution of the distribution of the phytoplankton population during one bloom cycle, whereas in Fig. 3 one may observe the nature of the oscillatory bloom in the mean population values of phytoplankton and zooplankton. The initial excitation is due to the absence of zooplankton in the eddies and, as before, the bloom propagates via diffusion throughout the domain. The main difference with the former scenario is that the expanding phytoplankton wave is not maintained in the vortices so the bloom decays and returns to the quiescent determination before the process is repeated.

What is fascinating is that the oscillatory regime is the most physically realistic scenario, as phytoplankton species are usually close to neutrally buoyant and zooplankton are slightly more dense than the surrounding ocean. However, notice that in the results shown here the value of the inertia parameter α from its dimensionless value ($A = 6$) is much smaller than what would be considered a realistic situation[19]. In a further work presented elsewhere [20] we adjust the value of the inertia parameter, obtaining qualitatively similar results that those ones presented here. Regardless of whether we use one or another value for α, we have corroborated that there are measurable qualitative differences between blooms involving zooplankton species of various sizes/densities, as it is reported in the experimental studies. However, a complete description of the problem would lead to a very complex model where, probably, the values of the inertial parameters and the material characteristics of the organisms would depend on time: $\alpha_i(t), R_i(t)$.

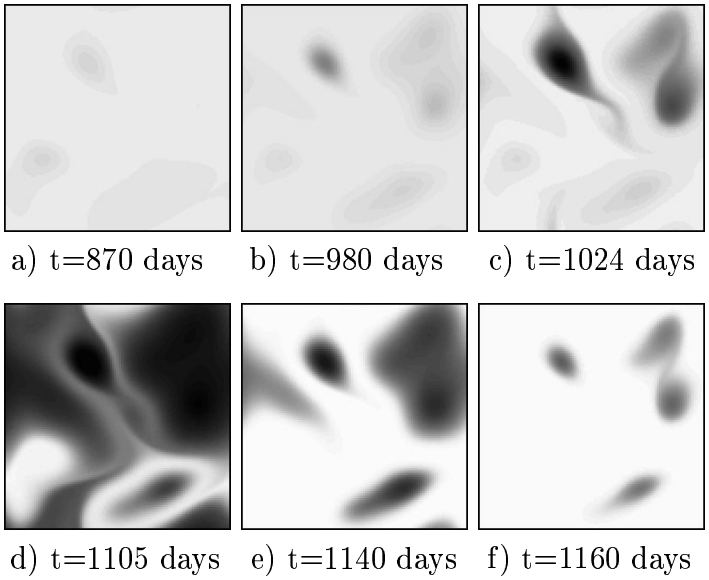

FIGURE 2. Snapshots of the phytoplankton population during the oscillatory bloom. Gray-scales as before.

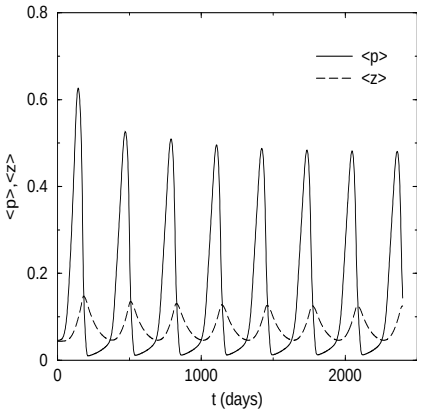

FIGURE 3. Oscillatory bloom in the mean concentrations of phytoplankton and zooplankton.

CONCLUSIONS

In this work, we have presented a methodology to generate synthetic turbulent flows from white noise that can be easily implemented numerically. As a result we obtain a stochastic velocity field which enters in the equations as a multiplicative noise with a spatio-temporal structure. This makes the problem non Markovian which deserves new mathematical techniques [21]. As an example of the possible applications of this approach we have shown here the main features of the dispersion of nonpassive (inertial) particles under turbulent advection.

Applying these results and this metodology to the study of Plankton dynamics, we have demonstrated how inertial separation of phytoplankton and zooplankton, cou-

pled with excitable reaction dynamics, may contribute towards oceanic phytoplankton blooms and patchiness. Of particular interest was the oscillatory excitation, which occured in the most realistic inertial regime (neutrally buoyant phytoplankton and slightly heavy zooplankton). The period of this oscillation was approximately one year and occurred for a range of parameter values. The result is particularly intriguing due to the resulting annual period of the blooms, although we would emphasize that seasonal forcing is likely to play a great role. Such seasonal forcing would consist of variations in temperature, light, nutrients (due to mixing) or fluctuations in other components of the food-chain. However, with a minimal model and using experimentally determined values for the parameters, we obtain a natural period of almost one year, which may be further synchronized by the forcing. This self-initiating, periodic patch forming mechanism differs from other related work on advection enhanced blooms [17] as it requires no initial perturbation and is self-sustaining.

ACKNOWLEDGMENTS

The authors acknowledge the support of this research by the Ministerio de Educación y Cultura through Projects No. BFM2000-0624 and BXX2000-0638, and by the Comissionat per Universitats i Recerca de la Generalitat de Catalunya under Project No. 1999SGR00041. RMH and MAB gratefully acknowledge financial support from the EU Access to Research Infrastructure action of the *Improving Human Potential Programme*.

REFERENCES

1. A.S. Monin and A.M. Yaglom, *Statistical Fluid Mechanics* (MIT, Cambridge, MA, 1975).
2. W.D. McComb, *The Physics of Fluid Turbulence* (Oxford University, Oxford, 1990).
3. A.C. Martí, J.M. Sancho, F. Sagués and A. Careta, *Phys. Fluids* **9**, 1078 (1997).
4. R.H. Kraichnan, *Phys. Fluids* **13**, 22 (1970).
5. R. Reigada, A.C. Martí, F. Sagués, I.M. Sokolov and J.M. Sancho, *Phys. Rev. E* **62**, 4997 (2000).
6. R. Reigada, F. Sagués and J.M. Sancho, *Phys. Rev. E* **64**, 026307 (2001).
7. R. Reigada, F. Sagués, I.M. Sokolov, J.M. Sancho and A. Blumen, *Phys. Rev. Lett.* **78**, 741 (1997).
8. R. Reigada, F. Sagués and J.M. Sancho, *J. Chem. Phys.* **117**, 258 (1998).
9. A.C. Martí, F. Sagués and J. M. Sancho, *Phys. Fluids* **9**, 3851 (1997).
10. A. M. Lacasta, J. M. Sancho and F. Sagués, *Phys. Rev. Lett.* **75**, 1791 (1995).
11. M.R. Maxey and J.J. Riley, *Phys. Fluids* **26**, 883 (1983).
12. M.R. Maxey, *J. Fluid Mech.* **174**, 441 (1987).
13. P. J. S. Franks, *Limnol. Oceanogr.* **42**, 1297 (1997).
14. E.R. Abraham, *Nature* **39**, 577 (1998).
15. C.L. Folt and C.W. Burns, *TREE* **14** 300 (1999).
16. J.E. Truscott and J. Brindley, *Bull. Math. Biol.* **56**, 981 (1994).
17. Z. Neufeld, P.H. Haynes, V.C. Garçon and J.Sudre, *Geophys. Res. Lett.* **29**, 1029 (2002).
18. A. Okubo, *Deep-Sea Research* **18**, 789 (1971).
19. K.D. Squires and H. Yamazaki, *Deep-Sea Research I* **42**, 1989 (1995).
20. R. Reigada, R.M. Hillary, M.A. Bees, J.M. Sancho and F. Sagués, (*in preparation*).
21. J.M. Sancho, M.A. Santos, S. Alonso and F. Sagués, (*in this volume*).